Thickness-dependent magnetoelasticity and its effects on perpendicular magnetic anisotropy in Ta/CoFeB/MgO thin films

P. G. Gowtham, G. M. Stiehl, D. C. Ralph, and R. A. Buhrman

Phys. Rev. B **93**, 024404 — Published 11 January 2016

DOI: 10.1103/PhysRevB.93.024404

Thickness-Dependent Magnetoelasticity and its Effects on Perpendicular Magnetic Anisotropy in Ta|CoFeB|MgOThin Films

P.G. Gowtham[1], G.M. Stiehl[1], D.C. Ralph,[1,2] and R.A. Buhrman[1]

[1]Cornell University, Ithaca, New York, 14853, USA

[2]Kavli Institute at Cornell, Ithaca, New York, 14853, USA

Abstract

We report measurements of the in-plane magnetoelastic coupling in both as-deposited and annealed ultra-thin Ta|CoFeB|MgO layers as a function of uniaxial strain, conducted using a four-point bending apparatus. While as-deposited samples show only a weak dependence of the magnetoelastic coupling on the CoFeB layer thickness in the ultrathin regime (< 2 nm), we observe the onset of a strong thickness dependence upon annealing. This dependence can be modeled as arising from a combination of effective surface and volume contributions to the magnetoelastic coupling. We point out that if similar thickness dependence exists for magnetoelastic coupling in response to biaxial strain, then the standard Néel model for the magnetic anisotropy energy acquires a term inversely proportional to the magnetic layer thickness. This contribution can significantly change the overall magnetic anisotropy, and provides a natural explanation for the strongly nonlinear dependence of magnetic anisotropy energy on magnetic layer thickness that is commonly observed for ultrathin annealed CoFeB|MgO films with perpendicular magnetic anisotropy.

Ultra-thin CoFeB|MgO films can possess strong perpendicular magnetic anisotropy (PMA). This observation is of great interest for non-volatile magnetic memory technologies because PMA is required for achieving thermal stability and low write currents at high densities[1]. The total effective anisotropy energy per unit area $K_{eff}t_{eff}$ is commonly analyzed using the Néel model[2], including surface (K_s) and volume (K_V) contributions to the magnetic anisotropy together with demagnetization effects:

$$K_{eff}t_{eff} = K_s - \left(2\pi M_s^2 - K_V\right)t_{eff}. \quad (1)$$

Here t_{eff} is the effective thickness of the magnetic layer excluding any dead layer, and $K_{eff}t_{eff} > 0$ corresponds to PMA. However, this simple form generally provides a poor description for the measured thickness dependence of magnetic anisotropy in ultra-thin CoFeB|MgO films possessing PMA. Whereas Eq. (1) predicts a simple linear increase in $K_{eff}t_{eff}$ as a function of decreasing t_{eff} (when $2\pi M_s^2 - K_V > 0$), the measured dependence in films with PMA is often strongly nonlinear, with $K_{eff}t_{eff}$ exhibiting a maximum as a function of decreasing t_{eff} and with the PMA eventually being lost for t_{eff} sufficiently small[3–9]. See, *e.g.*, the data corresponding to the annealed sample in Fig. 1. Non-idealities such as Ta diffusion to the CoFeB|MgO interface during annealing[5,6] are possible reasons for this behavior, but here we suggest that a thickness-dependent magnetoelastic coupling can contribute significantly to this nonlinear $K_{eff}t_{eff}$ *vs.* t_{eff} dependence observed for ultra-thin CoFeB|MgO with PMA, and may be the dominant explanation for the non-linear behavior.

We investigated Ta(6 nm)/$Co_{40}Fe_{40}B_{20}$(t_{CoFeB})/MgO(2.2 nm)/Hf(1 nm) multilayers deposited by magnetron sputtering onto 375 μm-thick Si wafers with 500 nm of thermal oxide, and with t_{CoFeB} ranging from 0.7 to 2.0 nm. Details of our film growth are provided in the Supplementary Material (SM). One set of wafers were used for magnetometry. Another set of samples were patterned into 20 μm ×100 μm microstrips using a series of photolithography and subsequent Ar ion milling steps. The microstrips were used for determining magnetoelastic couplings in the Ta|CoFeB|MgO|Hf system. We annealed a full thickness series of both magnetometry samples and microstrip samples at T = 300 °C for 1 hour in an in-plane field of 1.3 kOe and at a vacuum pressure of < 5×10^{-7} torr. The field anneal direction was along the current flow direction of the devices.

Magnetometry measurements on our as-deposited and annealed films were conducted at room temperature using a SQUID magnetometer. The magnetic moments per unit area M_{sheet} are plotted versus t_{CoFeB} in Fig. 2a. For both as-deposited and annealed samples, linear fits of M_{sheet} vs. t_{CoFeB} extrapolate to zero near $t_{CoFeB} = 0$, indicating a negligible magnetic dead layer thickness ($t_{eff} = t_{CoFeB}$). Previous studies of Ta|CoFeB samples have differed regarding the extent of any magnetic dead layers, with some indicating the existence of a dead layer[6,10] as thick as 0.5 nm after annealing and others reporting no dead layer[1,4,11]. Such variation suggests that the extent of any dead layer can depend on the precise choice of sputtering conditions, stack order, processing protocols, and base layer structure[11]. We note that cross-sectional scanning transmission electron microscopy of one of our multilayer samples indicates that the 6 nm Ta base layer is polycrystalline, while other work that found a 0.5 nm dead layer reported that the thinner, ~ 1 nm, Ta base used there appears to be amorphous. From the slopes of the fits in Fig.

2a, the CoFeB saturation magnetization is M_s = 1120 emu/cm^3 for the as-deposited samples and M_s =1380 emu/cm^3 after annealing. The rise in M_s is consistent with B segregation from the CoFe and partial crystallization of the CoFe layer during the annealing.

We characterized the effective anisotropy energy per unit volume K_{eff} by measuring the magnetization M as a function of applied magnetic field H both in (□) and out of (⊥) the sample plane for samples of each t_{eff} value (e.g., Fig. 2b), and extracted K_{eff} using the expression[12]

$$K_{eff} = M_s \left(\int_0^1 H_{\perp}(m_{\perp})\, dm_{\perp} - \int_0^1 H_{\square}(m_{\square})\, dm_{\square} \right), \qquad (2)$$

where $m_{\perp}$ and $m_{\square}$ are the normalized components of magnetization out-of-plane and in-plane. The results for $K_{eff}t_{eff}$ *vs.* t_{eff} are shown as symbols in Fig. 1 for both the as-deposited and annealed samples. The as-deposited samples display good agreement with the linear dependence predicted by the simple Néel model (Eq. (1)) with the fit parameters K_s = 0.3 erg/cm^2 and K_V = 1.6×10^6 erg/cm^3. However $K_{eff} < 0$ for all thicknesses (0.7 nm to 2 nm) of the as-deposited samples so that PMA is never achieved. After annealing, PMA is obtained in the thickness range 0.7 nm < t_{eff} < 1.2 nm, but as noted above this generation of PMA occurs simultaneously with a strongly nonlinear $K_{eff}t_{eff}$ *vs.* t_{eff} behavior in this t_{eff} range. The maximum value of anisotropy per unit area obtained was $K_{eff}t_{eff}$ = 0.26 erg/cm^2 at t_{eff} = 0.9 nm. A fit to Eq. (1) for the annealed samples in the range t_{eff} = 1.1 nm to 2.0 nm where $K_{eff}t_{eff}$ *vs.* t_{eff} is approximately linear yields K_s = 1.5 erg/cm^2 and K_V = 0.7×10^6 erg/cm^3.

Following this basic magnetic characterization, we measured the magnetoelastic coupling for the films with in-plane anisotropy using a four-point bend (4PB) strain tester (Fig. 3a). This geometry applies uniaxial strain on the top surface of the substrate, $\delta\varepsilon_{xx}^{top}$, that is uniform between the two inner loading pins and is completely determined by the spacing of the four loading points and the thickness of the substrate:[13,14]

$$\delta\varepsilon_{xx}^{top} = t_s\left(\delta h_{load}\right) / \left(\frac{2}{3}s_2^2 + s_1 s_2\right). \tag{3}$$

The quantity δh_{load} is the vertical displacement for the inner pins (a negative number in our experiment) and the other quantities are as defined in Fig. 3a. Here $\varepsilon_{xx} < 0$ corresponds to compression. We use the notation $\delta\varepsilon_{xx}$ rather than simply ε_{xx} because the CoFeB in Ta|CoFeB|MgO multilayer is, as indicated by K_V and as discussed below, strained even when $\delta h_{load} = 0$. For our geometry, s_1 = 14 mm, s_2 = 8 mm, and t_s = 375 μm. In the limit that the film stack thickness is much smaller than the substrate thickness and the bending is elastic, the mechanically applied strain in the CoFeB can be assumed to be the same as that at the top surface of the Si chip.

Our procedure for measuring the magnetoelastic coupling was to use a lock-in amplifier and Wheatstone bridge to perform a 2 point measurement of the anisotropic magnetoresistance (AMR) as a function of swept magnetic field for different fixed values of applied bending strain, using 5.3 mm × 45 mm device dies with the long axis along the x direction in Fig. 3b, perpendicular to the current direction in the sample. Each die was loaded with the long axis bridging the support pins of the 4PB apparatus, inside an electromagnet capable of applying a magnetic field in the x direction. For the annealed in-plane magnetized samples (t_{eff} > 1.2 nm),

the magnetic easy axis was set along the y-direction by the field orientation during annealing. For the as-deposited samples the y-axis was made the easy axis by applying a sufficient compressive strain in the x-direction (usually $|\delta\varepsilon_{xx}| > 0.05\%$). For both types of samples, therefore, the applied magnetic field was oriented along the in-plane hard axis, and produced a non-hysteretic rotation of the magnetization. Under these conditions, the AMR curve serves as a faithful representation of the in-plane rotation angle φ for the average magnetization, with $R(\varphi) = R_0 + \Delta R \sin^2 \varphi$. The resistance is a minimum when the magnetization is saturated along the x-axis.

Because of the magnetoelastic coupling, the application of a compressive bend strain alters the shape of the AMR curve by changing the in-plane magnetic anisotropy energy. Figure 3c shows the measured AMR for a t_{eff} = 1.7 nm sample with $\delta\varepsilon_{xx}$ ranging from 0 to -0.095% in increments of -0.0065%. The AMR curves are normalized for each value of strain by mapping the (large-field) saturated resistance value to 0 and the (zero-field) maximum resistance value to 1. With the identification that the normalized x-component of magnetization is $m_x = \cos[\arcsin[\sqrt{R_{norm}}]]$, the AMR measurements can then be transformed to yield $H_x(m_x)$ *vs.* m_x curves (shown in Fig 3d), from which the in-plane uniaxial magnetoelastic coupling $B_{eff}^{uniaxial}$ multiplied by the strain can be calculated as:[15]

$$\left(\delta\varepsilon_{xx}\right) B_{eff}^{uniaxial} = \frac{\frac{3}{4} M_s \left(\int_{m_1}^{m_2} H_x(m_x, \delta\varepsilon_{xx}) dm_x - \int_{m_1}^{m_2} H_x(m_x, 0) dm_x \right)}{(m_2^2 - m_1^2)} \equiv \Lambda. \qquad (4)$$

Here m_1 and m_2 are normalized magnetization points in the H_x *vs.* m_x curve that are used as limits of integration (we use $m_1 = 0.4$ and $m_2 = 0.8$). Equation (4) holds under the assumption

that the Poisson ratio $\nu = 1/3$ (previous experiments report $0.25 < \nu < 0.4$ for metals in thin film form[16–18] and in bulk[19,20]) and that the CoFeB is an isotropic medium in the plane of the film. The latter assumption should be accurate for our samples as no in-plane texturing is expected in annealed Ta/CoFeB/MgO multilayers, although there is strong grain-by-grain out-of-plane texturing at the CoFeB|MgO interface.[21] We determine $B_{eff}^{uniaxial}$ by fitting Λ (the right hand side of Eq. (4)) *vs*. $\delta\varepsilon_{xx}$ to a straight line for each sample and evaluating the slope as shown in the inset of Fig 3d.

Measurements of the in-plane magnetoelastic coupling for the samples in which the magnetic anisotropy is in plane are shown in Fig. 4 for both the as-deposited and annealed Ta|CoFeB|MgO thin films. For the as-deposited samples, $B_{eff}^{uniaxial}$ is approximately constant, near -4 $\times 10^7$erg/cm^3 for all values of t_{eff}. As will be discussed below, if we assume that the volume anisotropy of the as-deposited sample, $K_V = 1.6 \times 10^6$ erg/cm^3, arises only from a biaxial elastic strain $K_V = B_{eff}^{biaxial} \varepsilon_{biaxial}^{as-deposited}$ (where $B_{eff}^{biaxial}$ is the component of the magnetoelastic tensor coupling to biaxial strains), the measured uniaxial magnetoelastic constant $B_{eff}^{uniaxial} \approx$ - 4 $\times 10^7$ erg/cm^3 suggests a large, and an approximately thickness-independent, biaxial compressive strain $\varepsilon_{biaxial}^{as-deposited}$ in the as-deposited samples. To estimate this strain we assume that

$$B_{eff}^{biaxial} \approx B_{eff}^{uniaxial} + B_{eff}^{13}, \tag{5}$$

where B_{eff}^{13} is the term that connects the magnetic free energy to strains perpendicular to the sample plane.[15] This relationship is appropriate for the condition of isotropy in the sample plane and a Poisson ratio $\nu \approx 1/3$, within the typical range found for metals. For purposes of

estimation here we can also assume $B_{eff}^{13} \approx B_{eff}^{uniaxial}$, which is appropriate for an isotropic system, such as the amorphous as-deposited film. This analysis indicates that $\varepsilon_{biaxial}^{as-deposited} \approx -0.02$, which is consistent with the strong compressive strain that is common in sputter-deposited refractory metal films.[22]

After annealing, our results show that, while the volume anisotropy is substantially reduced, the magnitude of $B_{eff}^{uniaxial}$ is considerably larger and has a pronounced dependence on t_{eff}, changing by 60 % between t_{eff} = 1.3 and 2.0 nm. The transition from a $B_{eff}^{uniaxial}$ that is approximately constant in thickness for the as-deposited samples to a $B_{eff}^{uniaxial}$ that is considerably larger and strongly thickness dependent is unexpected. We surmise that this transition may be connected to microstructural changes occurring in the CoFeB layer as the film transitions from fully amorphous to a state of partial crystallization templated off of MgO grains. Furthermore, dependence for the annealed case fits well to the functional form $B_{eff}^{uniaxial} = (B_s^u / t_{eff}) + B_V^u$, suggesting that in the annealed samples there is both a strong volume magnetoelastic coupling B_V^u = -1.5×10^8 erg/cm^3 and strong effective interfacial magnetoelastic coupling B_s^u = +12.1 erg/cm^2. One possible mechanism for an apparent interfacial magnetoelastic coupling term is a large second-order term D in the volume magnetoelastic coupling, $B_{eff}^{uniaxial} = B_V^0 + D\varepsilon$, in combination with a strongly thickness-dependent strain in the annealed samples, as observed in coherent, epitaxial bilayers with a strong crystalline mismatch[22]. Alternatively or in addition, another possible mechanism for the observed thickness dependence is that the same interface electronic effect (i.e. Fe-3d/O 2p hybridization)[24,25] at the CoFeB|MgO interface responsible for the strong PMA in the thin annealed and partially crystallized CoFe(B) films[26–32] also contributes

an interface-like term to the effective magnetoelasticity of the annealed samples. Future ab-initio work to determine the interfacial magnetoelastic coupling arising at the CoFeB|MgO due to surface electronic effects as well as experiments designed to isolate this magnetoelastic contribution arising from interfacial electronic effects would be very interesting.

If the strain in annealed CoFeB|MgO samples is thickness-dependent in the presence of a strongly thickness-dependent magnetoelasticity, the magnetic anisotropy will be strongly altered. To analyze this effect, we employ a generalization of the Néel model that explicitly takes into account the magnetoelastic contribution to the magnetic energy[32,33]:

$$K_{eff}t_{eff} = K_s^0 + \left[K_V^0 - \left(2\pi M_s^2\right) + B_{eff}^{biaxial}\left(t_{eff}\right)\varepsilon_{biaxial}\left(t_{eff}\right)\right]t_{eff}. \quad (6)$$

Here K_s^0 and K_V^0 are the surface and volume magnetoelastic couplings at zero strain. We consider the case relevant to CoFeB|MgO films without in-plane texture, where the strain associated with growth and annealing should be biaxial, and for simplicity we assume that the average strain variation with CoFeB thickness can be approximated as

$$\varepsilon_{biaxial}\left(t_{eff}\right) \approx \varepsilon_0^{biaxial} + \left(\gamma_{biaxial} / t_{eff}\right) \quad (7)$$

over the thickness range t_{CoFeB} = 0.7 – 2.0 nm employed in our study. The precise functional form is not essential for our conclusions (see the SM for further discussion of this point). The expression we have chosen to model the variation in strain has the virtue of yielding a particularly simple extension of the Néel form for $K_{eff}t_{eff}$. Generally, the effect of the thickness-dependent magnetoelasticity on the magnetic anisotropy requires that the strain in the CoFeB layer increases strongly after annealing with decreasing t_{CoFeB} for the thinner films in the range studied, and varies much less strongly or not at all for the samples with t_{CoFeB} > 1.2 nm. We note

that $B_{eff}^{biaxial}$ (Eq. (5)) involves a different combination of magnetoelastic tensor elements than $B_{eff}^{uniaxial}$. Neither B_{eff}^{13} nor $B_{eff}^{biaxial}$ have been measured for Ta|CoFeB|MgO samples, either as-deposited or annealed. However, as long as the overall magnetoelastic coupling $B_{eff}^{biaxial}$ has a significant interface term, with $B_{eff}^{biaxial} \approx (B_s^b / t_{eff}) + B_V^b$, then it follows from Eq. (6) that the total magnetic anisotropy per unit area should approximately possess a simple, separable functional form

$$K_{eff} t_{eff} = (K_V^f - 2\pi M_s^2) t_{eff} + K_s^f + \frac{K_3}{t_{eff}}, \tag{8}$$

containing an effective volume term with coefficient $K_V^f = K_V^0 + B_V^b \varepsilon_0^{biaxial}$, an effective surface term with coefficient $K_s^f = K_s^0 + B_V^b \gamma_{biaxial} + B_s^b \varepsilon_0^{biaxial}$, and a term scaling as t_{eff}^{-1} with coefficient $K_3 = B_s^b \gamma_{biaxial}$. The dashed line in Fig. 1 is a 3-parameter fit of Eq. (7) to the data for our annealed Ta|CoFeB|MgO samples, with $K_V^f - 2\pi M_s^2 = (-1.77 \pm 0.03) \times 10^7$ ergs/cm^3, $K_s^f = +3.25 \pm 0.03$ ergs/cm^2, and $K_3 = (-1.28 \pm 0.03) \times 10^{-7}$ erg/cm.

An accurate quantitative analysis of the different contributions to the anisotropy requires knowing the value of $B_{eff}^{biaxial}$ or equivalently both $B_{eff}^{uniaxial}$ and B_{eff}^{13}. In principle, $B_{eff}^{biaxial}$ can be measured by a biaxial strain test (e.g. a ring-on-ring test). However, for purposes of estimation here we will assume $B_{eff}^{13} \approx B_{eff}^{uniaxial}$, so that $B_{eff}^{biaxial}\left(t_{eff}\right) \approx 2 B_{eff}^{uniaxial}\left(t_{eff}\right)$. This assumption is rigorous in systems with full isotropy or cubic symmetry, but will not be rigorous for our

samples due to out-of-plane texturing of the CoFeB film and symmetry breaking at the CoFeB|MgO interface. Given our determination that $B_s^u = +12.1$ erg/cm^2 provides a good fit to the measured t_{eff} dependence of $B_{eff}^{uniaxial}$ of the annealed samples (Fig. 4), an explanation of the nonlinearity in $K_{eff}t_{eff}$ versus t_{eff} entirely in terms of thickness-dependent magnetoelastic coupling then requires that $\gamma_{biaxial}$ have the value $\gamma_{biaxial} \approx K_3/(2B_s^u) = -0.053 \pm .002$ nm, and that $\varepsilon_0^{biaxial} \approx K_V^f/(2B_V^u) = 0.019$, under the assumption $K_V^0 = 0$. The negative sign of $\gamma_{biaxial}$ here corresponds to a greater magnitude of compressive strain for thinner CoFeB films and a lower compressive strain ($\varepsilon_{biaxial} \leq -0.016$) as the CoFeB film gets into a higher thickness range 1.5 nm $< t_{eff} <$ 2 nm. The magnitude that we estimate for $\gamma_{biaxial}$ corresponds to a total change in average CoFeB film strain over the thickness range of our anisotropy measurements (0.7 – 2.0 nm) of $\Delta\varepsilon^{biaxial} = 0.05$.

The presence of compressive strains in the CoFeB film estimated by the preceding analysis conflicts with strains predicted from consideration of the equilibrium lattice mismatch between hetero-epitaxial thin film layers of MgO and CoFe at a coherent interface. If we assume bulk equilibrium lattice constants, the CoFeB (MgO) should be under tensile (compressive) rather than the compressive (tensile) stress[6,35]. However the available experimental evidence agrees with our conclusions regarding the presence of compressive strain. Recent X-ray diffraction measurements on CoFeB(6nm)/MgO(2nm) multilayers have reported that the equilibrium lattice spacing of bulk MgO is not observed in these layers, but rather that the MgO lattice is considerably expanded and thus is under tensile stress, with this expansion decreasing with higher annealing temperatures (250 ºC to 400 ºC). The tensile strain can potentially be

attributed to point defects, which are generally found to expand the lattice of non-stoichiometric oxides.[36,37] The X-ray work also reports that the annealing process results in the formation of textured "nanopipes"[21] as crystalline CoFe grains nucleate at the CoFeB|MgO interface. The process occurs through crystallization templating of the CoFeB off the MgO surface and is accomplished by B out-diffusion. The study shows that these nano-columnar, partially crystallized CoFe grains are under high compressive biaxial strain.[38] The CoFe lattice parameter reported is compressed more than 3% below the bulk equilibrium value for a 300 ºC annealed multilayer, resulting in an average lattice parameter difference between the MgO and CoFe greater than 7% (4.5%) for a 300 ºC (400 ºC) CoFeB(6 nm)|MgO(2 nm) sample.

We surmise therefore that coherent heteroepitaxy is not the dominant factor in determining the strain configuration adjacent to these thin CoFe|MgO bi-layers as it cannot be responsible for the compressive strain on the CoFe grains as observed by this X-ray study, and as needed to account for the thickness-dependent magnetic anisotropy in terms of a interfacial magnetoelastic effect as we are proposing here. We speculate that the CoFe compressive strain arises instead from the B displacement during the nucleation and growth of the textured CoFe|MgO nanopipes that are required for high TMR, and presumably for strong interfacial anisotropy.

In summary, we have measured the magnetoelastic coupling in annealed Ta|CoFeB|MgO samples for in-plane uniaxial strains, finding a strong dependence on the thickness of the CoFeB layer that can be modeled in terms of large volume and surface contributions to the magnetoelastic coupling. We suggest that a thickness-dependent magnetoelastic coupling and thickness-dependent elastic strain can together have a significant influence on the strength and thickness dependence of PMA in annealed Ta|CoFeB|MgO samples. In particular, thickness-

dependent magnetoelastic coupling provides a natural explanation for the functional form of the nonlinearity commonly observed for thin magnetic layers with PMA in their curves of $K_{eff}t_{eff}$ vs. t_{eff}. More detailed measurements of the biaxial magnetoelastic coupling and characterization of the strain distribution in ultrathin CoFeB|MgO bilayers are thus warranted. A clear understanding of the strain distribution in nanocolumnar CoFeB formed by templating off of nanocrystalline MgO, and the role that B diffusion and various NM underlayers are playing in this distribution are currently lacking. A clear picture of the interplay between the biaxial magnetoelastic coupling, strain distribution, and materials physics/chemistry in NM|CoFeB|MgO systems would allow for deeper insight into the behavior of the PMA in these systems, and potentially offers new routes for tailoring the PMA for technological applications.

Acknowledgements

We thank R.B. van Dover for useful discussions and Nathan Ellis for aiding us in the design of the 4PB setup. We also thank G.E. Rowlands, L.H. Villela-Leao, J. Park, Y.X. Ou, and S.V. Chakram for assistance. This research was supported by ONR, ARO, and NSF (DMR-1406333), and made use of the Cornell Center for Materials Research Shared Facilities which are supported through the NSF MRSEC program (DMR-1120296). This work was also performed in part at the Cornell NanoScale Facility, a member of the National Nanotechnology Infrastructure Network, which is supported by the National Science Foundation (Grant ECCS-15420819).GMS acknowledges support by a National Science Foundation Graduate Research Fellowship under Grant No. DGE-1144153.

References

1. Ikeda, S. *et al.* A perpendicular-anisotropy CoFeB-MgO magnetic tunnel junction. *Nat. Mater.* **9,** 721–4 (2010).

2. Neel, L. L'approche a la saturation de la magnetostriction. *J. Phys. Rad.* **15,** 376 (1954).

3. Worledge, D. C. *et al.* Spin torque switching of perpendicular Ta/CoFeB/MgO-based magnetic tunnel junctions. *Appl. Phys. Lett.* **98,** 022501 (2011).

4. Liu, T., Cai, J. W. & Sun, L. Large enhanced perpendicular magnetic anisotropy in CoFeB/MgO system with the typical Ta buffer replaced by an Hf layer. *AIP Adv.* **2,** 032151 (2012).

5. Miyakawa, N., Worledge, D. C. & Kita, K. Impact of Ta Diffusion on the Perpendicular Magnetic Anisotropy of Ta/CoFeB/MgO. *IEEE Magn. Lett.* **4,** 1000104 (2013).

6. Sinha, J. *et al.* Enhanced interface perpendicular magnetic anisotropy in Ta|CoFeB|MgO using nitrogen doped Ta underlayers. *Appl. Phys. Lett.* **102,** 242405 (2013).

7. Den Broeder, F. J. A., Kuiper, D., van de Mosselaer, A. P. & Hoving, W. Perpendicular Magnetic Anisotropy of Co-Au Multilayers Induced by Interface Sharpening. *Phys. Rev. Lett.* **60,** 2769–2772 (1988).

8. Den Broeder, F. J. A., Hoving, W. & Bloemen, P. J. H. Magnetic anisotropy of multilayers. *J. Magn. Magn. Mater.* **93,** 562–570 (1991).

9. Jungblut, R., Johnson, M. T., aan de Stegge, J., Reinders, A. & den Broeder, F. J. A. Orientational and structural dependence of magnetic anisotropy of Cu/Ni/Cu sandwiches: Misfit interface anisotropy. *J. Appl. Phys.* **75,** 6424 (1994).

10. Khalili Amiri, P. *et al.* Switching current reduction using perpendicular anisotropy in CoFeB-MgO magnetic tunnel junctions. *Appl. Phys. Lett.* **98,** (2011).

11. Yamanouchi, M. *et al.* Dependence of magnetic anisotropy on MgO thickness and buffer layer in Co20Fe60B20-MgO structure. *J. Appl. Phys.* **109,** 07C712 (2011).

12. Johnson, M. T., Bloemen, P. J. H., den Broeder, F. J. . & de Vries, J. J. Magnetic anisotropy in metallic multilayers. *Rep. Prog. Phys* **59,** 1409–1458 (1996).

13. Hollenberg, G. W., Terwilliger, G. R. & Gordon, R. S. Calculation of Stresses and Strains in Four-Point Bending Creep Tests. *J. Am. Ceram. Soc.* **54,** 196–199 (1970).

14. Weihnacht, V., Bru□ckner, W. & Schneider, C. M. Apparatus for thin-film stress measurement with integrated four-point bending equipment: Performance and results on Cu films. *Rev. Sci. Instrum.* **71,** 4479 (2000).

15. O'Handley, R. C., Song, O.-S. & Ballentine, C. A. Determining thin-film magnetoelastic constants. *J. Appl. Phys.* **74,** 6302 (1993).

16. Zhao, J.-H., Du, Y., Morgen, M. & Ho, P. S. Simultaneous measurement of Young's modulus, Poisson ratio, and coefficient of thermal expansion of thin films on substrates. *J. Appl. Phys.* **87,** 1575 (2000).

17. Kalkman, A. J., Verbruggen, A. H. & Janssen, G. C. A. M. Young's modulus measurements and grain boundary sliding in free-standing thin metal films. *Appl. Phys. Lett.* **78,** 2673–2675 (2001).

18. Villain, P., Renault, P. O., Goudeau, P. & Badawi, K. F. X-ray diffraction measurement of the Poisson's ratio in Mo sublayers of Ni/Mo multilayers. *Thin Solid Films* **406,** 185–189 (2002).

19. Greaves, G. N., Greer, A. L., Lakes, R. S. & Rouxel, T. Poisson's ratio and modern materials. *Nat. Mater.* **10,** 986–986 (2011).

20. Smithells, C. J. *Metals Reference Book*. (Butterworths Scientific Publications, 1955).

21. Choi, Y. S., Tsunekawa, K., Nagamine, Y. & Djayaprawira, D. Transmission electron microscopy study on the polycrystalline CoFeB⁄MgO⁄CoFeB based magnetic tunnel junction showing a high tunneling magnetoresistance, predicted in single crystal magnetic tunnel junction. *J. Appl. Phys.* **101,** 013907 (2007).

22. Thornton, J. & Hoffman, D. Stress-related effects in thin films. *Thin Solid Films* **171,** 5–31 (1989).

23. Tian, Z., Sander, D. & Kirschner, J. Nonlinear magnetoelastic coupling of epitaxial layers of Fe, Co, and Ni on Ir(100). *Phys. Rev. B* **79,** 024432 (2009).

24. Sun, S. & O'Handley, R. Surface magnetoelastic coupling. *Phys. Rev. Lett.* **66,** 2798–2801 (1991).

25. Song, O., Ballentine, C. A. & O'Handley, R. C. Giant surface magnetostriction in polycrystalline Ni and NiFe films. *Appl. Phys. Lett.* **64,** 2593 (1994).

26. Worledge, D. C., Hu, G., Abraham, D. W., Trouilloud, P. L. & Brown, S. Development of perpendicularly magnetized Ta|CoFeB|MgO-based tunnel junctions at IBM (invited). *J. Appl. Phys.* **115,** 172601 (2014).

27. Yang, H. X. *et al.* First-principles investigation of the very large perpendicular magnetic anisotropy at Fe|MgO and Co|MgO interfaces. *Phys. Rev. B* **84,** 054401 (2011).

28. Linn, T. & Mauri, D. U.S. Patent 6841395 B2. *U.S. Patent* 1–5 (2013).

29. Khoo, K. H. *et al.* First-principles study of perpendicular magnetic anisotropy in CoFe/MgO and CoFe/Mg_{3}B_{2}O_{6} interfaces. *Phys. Rev. B* **87,** 174403 (2013).

30. Ahn, S. & Beach, G. S. D. Crossover between in-plane and perpendicular anisotropy in Ta / Co x Fe 100- x / MgO films as a function of Co composition. *J. Appl. Phys.* **112,** 2011–2014 (2013).

31. Sokalski, V., Moneck, M. T., Yang, E. & Zhu, J.-G. Optimization of Ta thickness for perpendicular magnetic tunnel junction applications in the MgO-FeCoB-Ta system. *Appl. Phys. Lett.* **101,** 072411 (2012).

32. Lam, D. D. *et al.* Composition Dependence of Perpendicular Magnetic Anisotropy in. *J. Magn.* **18,** 5–8 (2013).

33. Bochi, G., Song, O. & O'Handley, R. Surface magnetoelastic coupling coefficients of single-crystal fcc Co thin films. *Phys. Rev. B* **50,** 2043–2046 (1994).

34. Bochi, G., Ballentine, C., Inglefield, H., Thompson, C. & O'Handley, R. Evidence for strong surface magnetoelastic anisotropy in epitaxial Cu/Ni/Cu(001) sandwiches. *Phys. Rev. B. Condens. Matter* **53,** R1729–R1732 (1996).

35. Butler, W., Zhang, X.-G., Schulthess, T. & MacLaren, J. Spin-dependent tunneling conductance of Fe|MgO|Fe sandwiches. *Phys. Rev. B* **63,** 054416 (2001).

36. Brooks, C. M. *et al.* Growth of homoepitaxial SrTiO[sub 3] thin films by molecular-beam epitaxy. *Appl. Phys. Lett.* **94,** 162905 (2009).

37. Freedman, D., Roundy, D. & Arias, T. Elastic effects of vacancies in strontium titanate: Short- and long-range strain fields, elastic dipole tensors, and chemical strain. *Phys. Rev. B* **80,** 064108 (2009).

38. Mukherjee, S. S. *et al.* Crystallization and grain growth behavior of CoFeB and MgO layers in multilayer magnetic tunnel junctions. *J. Appl. Phys.* **106,** 033906 (2009).

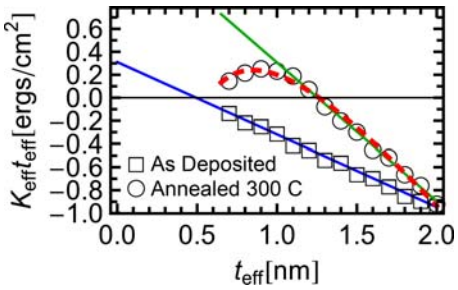

Figure 1. $K_{eff}t_{eff}$ vs. t_{eff} for the as-deposited and annealed Ta(6 nm)|$Co_{40}Fe_{40}B_{20}$(t_{CoFeB})|MgO(2.2 nm)|Hf(1 nm) thickness series. The $K_{eff}t_{eff}$ data for the as-deposited samples fit well to a Néel model with K_s ~0.3 ergs/cm^2. The annealed data are compared to a Néel model fit (solid green) and to a model including thickness-dependent magnetoelastic interactions (dashed red).

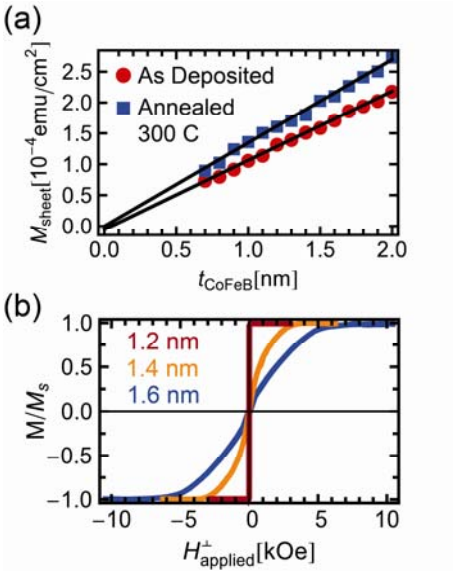

Figure 2. a) The magnetic moment sheet density M_{sheet} vs. nominal CoFeB film thickness for the as-deposited and annealed films. The slopes of linear fits to the data yield M_s = 1120 emu/cm^{3}and M_s = 1380 emu/cm^{3}for the as-deposited and annealed samples, respectively. No appreciable magnetic dead layers are found in our samples either as-deposited or after annealing. **b)** SQUID scans of annealed films with field oriented perpendicular to the film plane for t_{CoFeB} = 1.2, 1.4, and 1.6 nm. The transition to PMA occurs near 1.2 nm.

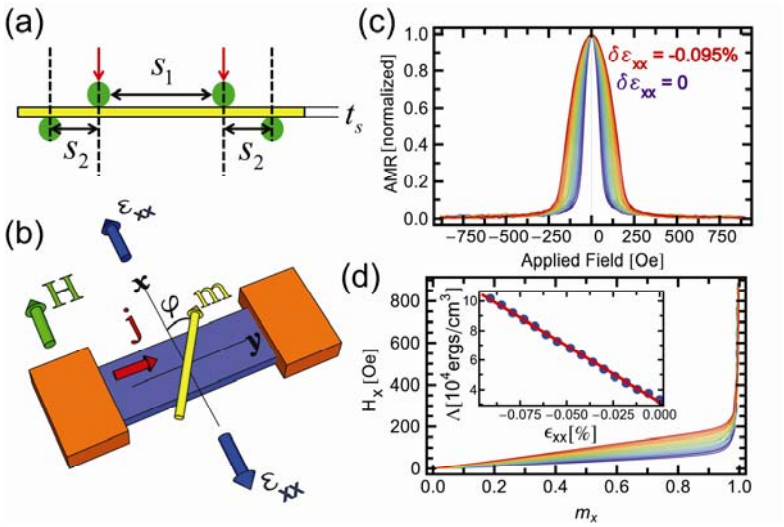

Figure 3.a) Schematic of the 4PB setup. **b)** Micro-wire device layout and geometry used for measuring AMR and extracting $B_{eff}^{uniaxial}$. **c)** Normalized MR hard axis curve series for an annealed device with t_{CoFeB} = 1.7 nm, as a function of increasing compressive strain. The $\delta\varepsilon_{xx}$ increment between each AMR sweep is –0.0065%. **d)** Conversion of AMR field sweeps to $H_x(m_x)$ curves. [**Inset:** Change in anisotropy energy density as a function of strain. The slope yields $B_{eff}^{uniaxial}$ ~ -7.6x10^7 erg cm^3 for the annealed sample with t_{CoFeB} = 1.7 nm.]

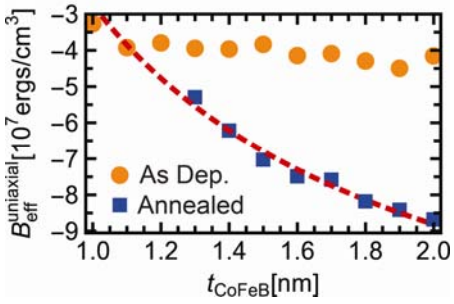

Figure 4. $B_{eff}^{uniaxial}$ vs. t_{CoFeB} for the samples as-deposited and annealed at 300 C for 1 hour. The dashed red line is a fit to the $B_{eff}^{uniaxial}$ vs. t_{CoFeB} data for the annealed series using the functional form $B_{eff}^{uniaxial} = (B_s^u / t_{eff}) + B_V^u$. The values B_s^u = +12.1 ergs/cm^2 and B_V^u = -1.5×10^8 ergs/cm^3 are extracted from the fit.